PHYSICAL REVIEW B VOLUME 56, NUMBER 23 15 DECEMBER 1997-I

High-energy Ce-$3d$ photoemission: Bulk properties of CeM_2 (M=Fe,Co,Ni) and Ce$_7$Ni$_3$

L. Braicovich
INFM (Istituto Nazionale di Fisica della Materia) and Dipartimento di Fisica del Politecnico, Piazza Leonardo da Vinci 32, 20133 Milano, Italy

N. B. Brookes and C. Dallera
ESRF, European Synchrotron Radiation Facility, Boîte Postale 220, 38043 Grenoble, France

M. Salvietti
Max Planck Institut für Mikrostrukturphysik, Weinberg 2, D-06120 Halle, Germany

G. L. Olcese
Dipartimento di Chimica e Chimica Industriale dell' Università, Via Dodecanneso 31, 16146 Genova, Italy

(Received 26 March 1997; revised manuscript received 9 July 1997)

We study the photon energy dependence of Ce-$3d$ photoemission in CeM_2 compounds (M=Fe,Co,Ni) and in Ce$_7$Ni$_3$ with measurements taken with synchrotron radiation in the photon energy range 1050–3850 eV. The results show a drastic increase of the bulk sensitivity at the higher energies due to the increase of the photoelectron escape depth. The spectra at 3850 eV are largely dominated by the bulk contribution, which is typically 85% of the total intensity in the CeM_2 compounds. The results allow us to obtain the bulk contribution to the spectra in CeM_2 with a procedure presented here and giving the fractional weights of the bulk f^0, f^1, and f^2 configurations. In the CeM_2 compounds a correlation is found between these spectral weights and the crystallographic data showing that the hybridization is nonmonotonic versus the atomic number of the transition metal. We discuss the results both in connection with an impurity model and with the available calculations in an itinerant model. Moreover, the results suggest that the bulk hybridization in CeM_2 systems with heavy transition metals has been probably underestimated up to now. [S0163-1829(97)06544-2]

I. INTRODUCTION

The electronic properties of cerium and of cerium compounds are one of the key topics in the physics of strongly correlated systems. In this field the application of electron spectroscopies has contributed important information, in particular, on the interaction between the Ce-$4f$ electrons and the surrounding environment through hybridization.[1–3] In these systems the surfaces are expected to have different properties with respect to the bulk so that a problem arises due to the surface versus bulk sensitivity of the various experimental methods. Ultraviolet photoemission spectroscopy, the traditional Al-$K\alpha$ XPS (x-ray photoemission spectroscopy), inverse photoemission in the ultraviolet and in the x-ray ranges give a mix of surface and bulk information in different proportions so that a quantitative comparison between the results of the different methods is not immediate. These problems were basically overlooked until it was shown experimentally[4,5] that the properties of Ce at the surface and in the bulk can be very different. In the systems studied in Refs. 4 and 5 the reduced coordination at the surface decreases the hybridization so that the surface Ce, in systems strongly hybridized in the bulk (often referred to as α-like systems in analogy with α-Ce), behave basically as Ce in weakly hybridized systems (referred to as γ-like systems in analogy with γ-Ce). A difference in behavior at the surface and in the bulk has also been pointed out by Liu *et al.*[6] in elemental Ce. The recovery of reliable bulk information from electron spectroscopy is still an open problem and the use of third-generation synchrotrons, as in the present case, can be very useful. The present paper is a step forward in this direction and deals with Ce-$3d$ XPS in the α-like compound sequence CeFe$_2$, CeCo$_2$, CeNi$_2$ and in a γ-like partner in the Ce-Ni phase diagram (Ce$_7$Ni$_3$). This last compound is presented merely for comparison since the main issue of the paper are α-like compounds. This work is based, as in the first contribution by Laubshat *et al.*,[4] on the kinetic-energy dependence of the photoelectron escape depth exploited to increase the relative bulk to surface sensitivity by using photons of increasing energy. We present Ce-$3d$ photoemission with photon energies up to about 4 keV so that the results are highly bulk sensitive. Since the cross sections are rapidly decreasing at high energies this experimental approach has been very difficult up to now because of the rather limited photon energy range accessible to the first works (typically 1100–1700 eV in Ref. 4). In high-energy photoemission the more natural and easier starting point is Ce-$3d$ XPS instead of valence photoemission. In fact, Ce-$3d$ lifetime broadening is considerable so that high-energy Ce-$3d$ XPS is easier since it does not require the resolution needed in valence photoemission. Nevertheless, Ce-$3d$ XPS gives significant information since the different configurations contributing to the spectra are very well separated by the Coulomb interaction.[1,2] By exploiting high-energy photoemission we introduce also a new method of data treatment in order to extract the bulk information. This approach is useful far from resonances where the disentangling of bulk versus surface can be more complicated due to possible differences in the surface and bulk resonances. Thus we do not cover the Ce L-threshold region. On the other hand, the resonant photoemission at the L threshold is interesting in itself and is another important issue in high-energy photoemission from Ce and Ce compounds.[7]

The three CeM_2 compounds (M = transition metal = Fe,Co,Ni) are typical examples of important $MgCu_2$-Laves phases. Although the object of theoretical work[8,9] the three compounds have not yet been studied completely even in conventional XPS. Data on Ce-$3d$ XPS from $CeCo_2$ and $CeNi_2$ are available[10] (however, without the possibility of disentangling safely surface and volume) while $CeFe_2$ data are lacking, to our knowledge. A specific reason of interest is the nonmonotonic lattice parameter with increasing Z providing a significant case in order to compare bulk spectroscopic information with crystallographic properties. In this connection we show a correlation already in the raw data in the bulk-sensitive regime. Besides that, we present an analysis to recover qualitative ground-state properties within the approximation of an impurity model[1,2] and we discuss the problem also in connection with the available information from an itinerant treatment.[8,9] The present results are also compared with the bulk information available in the literature on related systems leading to suggestions for further research.

The paper is organized as follows. The experimental information is given in Sec. II while an overview of the experimental results is given in Sec. III, including the relative weights of the various configurations in the bulk. The results are discussed in Sec. IV. The technical details of the data handling in order to extract the bulk information are given in Sec. V. The reader not interested in these details can go directly to the conclusions given in Sec. VI.

II. EXPERIMENT

The polycrystalline samples were prepared by induction melting from stoichiometric amounts of the pure components under Argon atmosphere. They were annealed for several days and checked by x-ray diffraction and microprobe analysis. The amount of unwanted phases is below 0.5%.

The measurements were made at the European Synchrotron Radiation Facility in Grenoble[11,12] using beamline ID12A with a double crystal monochromator (minimum energy$\cong$2 keV) and a side branch beamline (ID12B) based on a grating in the Dragon mounting working between 0.5 and 1.6 keV. Photoemission at $h\nu = 2660$ and 3850 eV has been measured at ID12A with a photon energy bandwidth of 0.8 eV while the other cases have been measured at ID12B (bandwidth between 1 eV at $h\nu = 1050$ and 1.4 eV at $h\nu = 1400$ eV). The photoemission spectra have been measured with a hemispherical spectrometer with entrance optics accepting $\pm 20°$ (Perkin Elmer PHI 3057 model with high-transmission Omega lens) with 60° incidence of the light with respect to the spectrometer input optics. We used normal photoemission in order to increase the bulk sensitivity. In the straight beamline a beryllium window was used to separate the vacuum of the chamber from the beamline to avoid contamination. The samples were cleaned *in situ* by scraping with a diamond file and were periodically cleaned about every two hours for precaution, always with reproducible results. The average acquisition time per spectrum is about 4 h.

The maximum photon energy in the experiment (3850 eV) was dictated by the upper kinetic energy measurable by the spectrometer in the standard configuration. This photon energy is sufficient to give spectra largely dominated by the bulk contribution. Our measurements taken with synchrotron radiation at the energy of the Al-$K\alpha$ line (1486.7 eV) are in excellent agreement with the literature on conventional Al-$K\alpha$ XPS.[10] In order to disentangle the bulk and surface contributions the use of the Ce-$3d$ photoemission excited at the Al-$K\alpha$ energy is more involved than in the other cases since the photoemission spectrum is superimposed to the broad distribution coming from the Ce-MNN Auger decay. Thus these measurements are not included in the present work.

III. OVERVIEW OF EXPERIMENTAL RESULTS

The Ce-$3d$ photoemission results from the four compounds are summarized in Fig. 1 giving an overview of the trend versus the photon energy and of the effect of chemical composition. All spectra are raw data (including background) and are normalized to the same height to show the lineshape changes. The binding energies are measured relative to that of the $3d_{5/2}$-f^1 peak, which is about 882 eV. The spectral assignments based on the f^0, f^1, and f^2 configurations are well known[1,2] and are given by the bars at the bottom of panel A. The difference between Ce_7Ni_3, which is γ-like, and the more hybridized Ce compounds (α-like) is, as expected, clearly seen. Moreover, in each of the three α-like Laves phases the spectra evolve at increasing photon energy towards a more α-like behavior since the spectra become more sensitive to the bulk. This is best shown by the increase of the f^0 and f^2 components on passing from the surface-sensitive regime at $h\nu = 1050$ eV (kinetic energy 135 eV) to the more bulk-sensitive regime at the maximum energy in this experiment ($h\nu = 3850$ eV–kinetic energy 2930 eV). This is consistent with the expectations[4–6,13] and allows an easy access to the bulk properties, as will be shown below.

The raw data show also differences within the α-like Laves phase family. This is better seen (Fig. 2) in the comparison between the bulk-sensitive spectra of the three compounds ($h\nu = 3850$ eV). A good indicator of the hybridization strength is the spectral intensity in the region between the two main f^1 peaks where two hybridization sensitive features ($3d_{5/2}$-f^0 and $3d_{3/2}$-f^2) overlap. In Fig. 2 this spectral region is presented with normalization of the three spectra to the same height of the $3d_{3/2}$-f^1 peak. The relative intensity in this region increases in the sequence $CeNi_2$,$CeFe_2$,$CeCo_2$ giving an hybridization trend nonmonotonic with the transition metal atomic number, which will be discussed later.

In the Laves phases the increase of the bulk sensitivity with increasing $h\nu$ is visible also in the comparison between the spectra taken $h\nu = 2660$ and 3850 eV. Thus even at high photon energies the surface contribution, although reduced, is not negligible and the spectrum at $h\nu = 3850$ eV is not completely bulklike. Hence, some data handling is still needed to obtain the bulk information. This will be done in Sec. V but we stress from the very beginning that in the

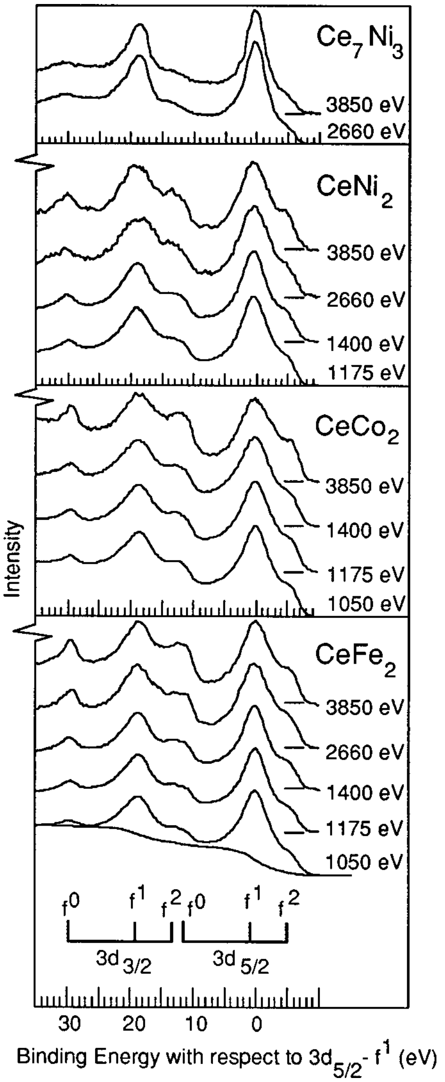

FIG. 1. Summary of Ce-3d photoemission results (raw data) from $CeFe_2$, $CeCo_2$, $CeNi_2$, and Ce_7Ni_3. The spectral assignments are given at the bottom. In the $CeFe_2$ case an example of the integral background is given.

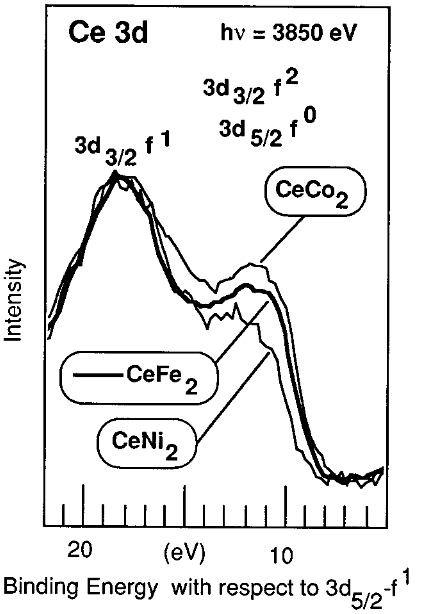

FIG. 2. Comparison between Ce-3d photoemission from the Laves phases $CeFe_2$, $CeCo_2$, $CeNi_2$ in the region comprising the $3d_{3/2}$-f^1 peak, the $3d_{3/2}$-f^2, and the $3d_{5/2}$-f^0 contributions. The spectra have been normalized to the same peak height to show the change of the line shape. Note the nonmonotonic change of the $3d_{3/2}$-f^2 and $3d_{5/2}$-f^0 intensity along the sequence $CeFe_2$,$CeCo_2$, $CeNi_2$.

high-energy region the surface effect is small and that the present data allow the recovery of the bulk properties with a high degree of confidence. In the limit of high kinetic energies the photoelectron escape depth (L) is much longer than the surface region thickness (s). It is reasonable that this thickness is of the order of 2 ML since the hybridization to the nearest neighbor is changed by the incomplete first-neighbor coordination shell and this in turn affects the second-neighbor coordination shell. In fact in the study of Ce overlayers onto Fe by using an Sm overlayer to suppress the Ce surface effects, Kierren *et al.*[14] have shown that a couple of layers is the typical depth scale affected by surface or interface effects. An independent argument showing that this thickness (hereafter referred to as ''surface thickness'') is about a couple of layers is given in Ref. 15 based on the comparison between resonant valence photoemission across the 3d and the 4d edges. Thus in our high-energy measurements the fractional weight of the surface component is of the order of (s/L). With the L values appropriate to the rare earths used in Ref. 6 this fractional weight is of the order of 15%. The small magnitude of this correction is the key point and explains why the bulk effects are well observed already in the raw data.

The Ce_7Ni_3 spectra taken at 2660 eV and at 3850 eV are identical within the statistics. This shows that a possible difference between bulk and surface in this case is much smaller than in α-like compounds, consistently with the initial arguments (Ref. 4). Due to the smallness of this possible effect the study of the separation of the bulk from the surface contributions is beyond the possibilities of the present work and the study of surface versus bulk effects in γ-like compounds is left for future investigations. These should be allowed in the present experimental setup[12] by an increase in sensitivity obtained with a stronger demagnification of the source onto the sample in the vertical direction. Thus the Ce_7Ni_3 spectra at lower energies are immaterial to the present discussion and were not measured.

A detailed discussion of the measured trends versus composition requires a knowledge of the weights of the various configurations in the bulk spectral functions. As mentioned above these are only marginally different with respect to the measurements at about 4 keV. However, the presentation of the data handling needed to recover the bulk information takes considerable space. Thus for clarity we anticipate the results and we postpone the presentation of the data treatment after the discussion of the results. The data treatment gives the weights of the bulk f^0,f^1,f^2 contributions one would measure with complete bulk sensitivity in Ce-3d photoemission (Table I—upper panel). The overall uncertainties discussed below (see Sec. V C) of the bulk values in the Laves phases are ± 0.01 (f^0 components), ± 0.02 (f^2 components), and ± 0.03 (f^1 components); these are the ranges of possible systematic errors and are not statistical errors

TABLE I. Summary of the bulk properties obtained from Ce-3d XPS. The upper panel gives the weights of the f^0, f^1, and f^2 configurations in the bulk spectral function (the values are close to the spectral weights measured with $h\nu = 3880$ eV and are obtained as explained in the text). The values obtained with an impurity model (see text) are given in the central panel (configurations in the theoretical XPS spectra) and in the lower panel (ground-state properties).

	$CeFe_2$	$CeCo_2$	$CeNi_2$	Ce_7Ni_3
Experimental XPS bulk values				
$f0$ weight	0.20 ± 0.01	0.21 ± 0.01	0.14 ± 0.01	0.05 ± 0.005
$f1$ weight	0.56 ± 0.03	0.52 ± 0.03	0.67 ± 0.03	0.86 ± 0.020
$f2$ weight	0.24 ± 0.02	0.27 ± 0.02	0.19 ± 0.02	0.09 ± 0.015
Model photoemission spectra				
$f0$ weight	0.20	0.21	0.15	0.05
$f1$ weight	0.56	0.52	0.67	0.86
$f2$ weight	0.24	0.27	0.18	0.09
Relative hybridization	1	1.2	0.6	0.21
Model ground state				
$f0$ weight	0.27	0.29	0.18	0.050
$f1$ weight	0.70	0.68	0.80	0.945
$f2$ weight	0.03	0.03	0.02	0.005
$4f$ occupation	0.76	0.74	0.84	0.955

fluctuating independently, since the inaccuracies combine to give always $f^0 + f^1 + f^2 = 1$.

IV. DISCUSSION

The discussion is divided into distinct parts. The first deals with the information one can extract from the bulk values of f^0, f^1, and f^2 in the XPS spectral functions *without using any model* so that the conclusions are not subject to the possible criticism connected with the use of models. In the second part we interpret our spectra in terms of the impurity model, which is a standard approach, to recover approximate information on the ground state. In this connection we discuss the results also in connection with the available information from band calculations (Refs. 8 and 9). Finally, we discuss the correlation between the macroscopic crystallographic properties, the excited-state properties given by the spectral functions, and the ground-state properties.

Let us begin with a comparison with the other available Ce-3d experimental information on Ce intermetallics. This is necessarily limited to the cases in which an attempt to disentangle surface and bulk contribution has been made.[16] Information is available on Laves phases with heavy M's. The substitution of a light M element with a heavier M is expected to increase the hybridization due to the strong increase of the spatial extension of the M-d wave function, which is in general greater than the increase of the interatomic distance.[17] In $CeRh_2$ a decomposition of the Cd 3d XPS in a surface and a bulk component has been presented recently[13] by using Mg-$K\alpha$ (1253.6 eV) and Al-$K\alpha$ (1476.7 eV) with a bulk f^0 contribution around 13–14%. This result is in qualitative agreement with the present findings but it is probably underestimated since the hybridization in $CeRh_2$ is expected to be greater than in $CeCo_2$ as explained above. It is likely that the inaccuracy of Ref. 13 is due to the limited photon energy range and to the difficulty of using Al-$K\alpha$ spectra as mentioned above. In Ref. 4 Laubshat *et al.* give results on $CeIr_2$ based on Ce 3d XPS in a wider but still rather limited energy range (1100–1700 eV) obtaining a f^0 weight that is the same, within the accuracy, as in our $CeFe_2$-$CeCo_2$. This is qualitatively correct but it is likely that in $CeIr_2$ the hybridization in the bulk has been somewhat underestimated in Ref. 4 since a greater hybridization is expected with Ir.[18] It would be interesting to investigate this and other related Laves phases with heavy M's in a wider photon energy interval.

It is interesting to compare the present $CeFe_2$ results with the recent results by Kierren and co-workers[14,19] on Ce-Fe interfaces. The authors studied Ce-3d photoemission from Ce overlayers onto Fe(100) and Fe(110) single crystals. To the purpose of the present discussion the interesting point is the large change of the spectral function upon continuation of the surface with another rare earth such as Sm. In this buried Ce monolayer we do expect a smaller hybridization than in bulk $CeFe_2$ since Ce is in contact with half a space of Sm not able to give the same hybridization as Fe. It is true that Sm-5d wave functions are much more extended than Fe 3d but they are too high in energy, Sm being formally d^0. In fact the measured bulk f^0 weight in $CeFe_2$ is 20% while in the buried monolayer it is about 15%.

In order to recover information on the ground state from Ce-3d XPS it is necessary to use models. The most widely used model is based on the assumption of treating the 4f states as a single impurity with an Anderson Hamiltonian.[1,2] This drastic assumption has been subject to criticism[20–23] in particular in the cases of very strong hybridization in which the lattice effects on the 4f states cannot be ruled out *a priori*. In the compounds treated here a conclusive assessment of the possibilities of this model cannot be made since a more detailed exploration of the bulk spectral functions from other spectroscopies is still lacking and it is known that the simultaneous use of different spectroscopy is important in the impurity model analysis. We use the model *only in qualitative terms to discuss* Ce-3*d* *XPS*. In this connection it is important to note that, in the final state, the attractive potential of the core hole has a dehybridizing effect due to the $4f$ shell contraction so that in α-like compounds this spectroscopy has a better chance of being described by the single impurity model than other spectroscopies (in particular, inverse photoemission where the added $4f$ electron has a hybridizing effect). Within these qualitative limits we are interested basically in the discussion of the trends of the spectral functions within the Laves phase family. We add also that the way of treating the ground-state properties of our Laves phases is open to controversy since the authors of Refs. 8 and 9 suggested that the ground state should be described in an itinerant model. For that reason we will also discuss briefly the link between the two descriptions.

With these precautions in mind we have made a fit of the spectral weights with a simple impurity model based on a semielliptical band to simulate the continuum, with hybridization independent of the configuration and without any correction for crystal field and multiplet effects. Since an accurate analysis of this kind on α-like Ce buried layer in contact with Fe has been published recently by Kierren *et al.*[14] we used as a reference this case that is related to $CeFe_2$ as discussed above. In the spirit of an approximate fitting we have used the same set of parameters as in Ref. 14, i.e., $U_{ff}=6.8$ eV, $U_{fc}=10.5$ eV, $\varepsilon_f=-1.2$ eV.[24] The semielliptical band has been taken 8 eV wide and its bottom has been put at -4 eV, consistently with the indications of the band calculations given in Ref. 8. Due to the strong similarity between the three Laves phases all above parameters are assumed to be the same in the three compounds, while the hybridization is changed to fit the different situations. We have made a fit of the spectrum by Kierren *et al.*[14] and after that we have increased the hybridization to fit the present spectral weights in the bulk, thus obtaining the values summarized in Table I, where the hybridizations are given as relative values with respect to $CeFe_2$. The hybridization of $CeFe_2$ is about two times that in the buried Ce monolayer of Ref. 14 with a decrease of the $4f$ occupation n_f from 0.818 (buried layer—Table I of Ref. 14) to 0.76 in bulk $CeFe_2$. Here we prefer to give the hybridization in relative terms since the absolute values, as it is well known, are dependent on the details in the implementation of the model in terms of the description of the continuum. To the purpose of the present discussion, it is more significant to think in terms of trends with respect to a reference value. The fit of the other compounds gives the values of Table I with a nonmonotonic trend of n_f in the three Laves phases at increasing atomic number of the $3d$ M. Within the limits discussed above the agreement between the model and the experiment is good in terms of the description of the weights in the spectral functions. Of course this agreement must not be overevaluated since, strictly speaking, it does not demonstrate that a single impurity description is fully adequate.

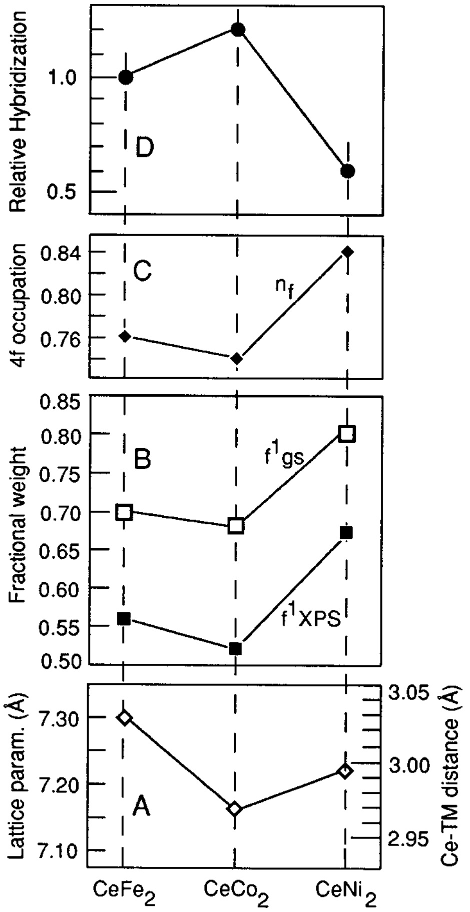

FIG. 3. Correlation between the crystallographic data and the photoemission results in the Laves phase sequence $CeFe_2$,$CeCo_2$, $CeNi_2$. Panel *A*: lattice parameters (left scale) and interatomic distances between Ce and the transition metal (right scale). Panel *B*: the weights of the f^1 configuration in the measured bulk XPS spectral function (black squares) and the f^1_{gs} ground state weights deduced with an impurity model as explained in the text (open squares). Panel *C*: the ground-state occupation n_f of Ce-$4f$ levels deduced with the impurity model. Panel *D*: the relative hybridization (with respect to $CeFe_2$ assumed as a reference), deduced with the impurity model from the fitting of Ce-$3d$ XPS.

Finally, it is interesting to compare the above results with the crystallographic data of the Laves phase family since it is known that they are not monotonic along the Fe-Co-Ni series. The relevant information is summarized in Fig. 3. In panel *A* the lattice parameter (left scale) and the Ce-*M* nearest-neighbor distance (right scale) are given. When the interatomic distance is smaller one expects a larger hybridization with a decrease of the $4f$ occupation and of f^1 weight and with an increase of the f^0 and f^2 weights. The trends of f^0 and f^2 in the raw spectra have been already shown in Fig. 2 and are correlated with the nonmonotonic trend of the lattice parameters. The weights f^1 in the measurements [black squares in Fig. 3(b)] obtained, without using models, by simply decomposing the spectra as in Sec. V A are also correlated with the trend of the lattice parameter in the sense that a minimum in $CeCo_2$ is seen. Some correlation is also seen with the estimated ground state values of f^1 [open squares in Fig. 3(b)] and, as a consequence, with the estimated $4f$ occupation [Fig. 3(c)]. The hybridization parameter in the model is given in panel *D* in relative terms with respect to $CeFe_2$ (black dots). The correlation with the crystallographic data is *qualitative* but, interestingly enough, it is seen *already in the raw data independently of any model.* Of course this argument cannot be pushed too far because the interatomic distances are only a qualitative indicator of the hybridization. In this connection a last interesting point is the interplay with the itinerant description of the ground state used in Refs. 8 and 9. By assuming a delocalized description we can consider the total $4f$ bandwidth as a qualitative indicator of the hybridization. The partial $4f$-derived density of states of Fig. 1 of Ref. 9 show a total $4f$ bandwidth that is clearly larger in $CeCo_2$ than in the other two compounds with a correlation with the trend of our hybridization parameter. In this sense there is a link between the itinerant and the impurity description. In effect the hybridization to be inserted in the impurity model should increase with the value of the $4f$ function on the Ce Wigner-Seitz sphere as suggested by Gunnarsson and Jepsen.[25] On the other hand, in an itinerant picture the bandwidth is increasing with this value, although nonlinearly, and this explains the existence of a correlation. Thus the present situation is consistent with the inherent link between the impurity and the itinerant descriptions given by the behavior of the $4f$ tails in the interatomic region. This also suggests that, in cases of strong hybridization, an itinerant ground state picture can probably give the trends of the typical parameters to be used in an approximate treatment of core excitations based on an impurity model.

V. DATA TREATMENT

Since the higher energy spectra are dominated by the bulk contribution and we are not interested in surface properties it is possible to introduce a new simple data treatment to recover bulk information. In the traditional approach the spectrum is decomposed with some best-fit procedure in a number of functions representing the subcomponents. Given a Ce site there are six components (f^0, f^1, and f^2 within each spin-orbit contribution), three of which are independent due to the constraints given by spin-orbit splitting and branching ratio. A spectrum containing a surface and a bulk contributions has thus to be decomposed in principle in 12 components (six from the bulk and six from the surface) and a background. Since the effects coming from the subsurface layer are in general present, the decomposition should be even more complicated and would imply 18 components (nine independent) and a background. Here instead of *functions* we are interested only in the weights of the bulk components f^0, f^1, and f^2, i.e., in *three numbers*. These numbers can be obtained rather directly from the high-energy data without a decomposition into subfunctions thus avoiding many difficulties, implicit assumptions, and uncertainties.

At each photon energy one obtains the fractional weights of the f^0, f^1, and f^2 components in a rather direct way as explained in Sec. VI A. Each weight is the sum of the bulk and of the surface contributions with an increasing sensitivity to the bulk at increasing $h\nu$. The next step is the use of the dependence of the measured weights on the photoelectron kinetic energy (Sec. VI B) showing a high-energy range in which $(s/L) \ll 1$, where s is the surface thickness and L the escape depth (this will be called ''asymptotic regime''). In this case it is rather easy to extract the bulk information with minor corrections to the measured weights. In what follows all examples refer to $CeFe_2$.

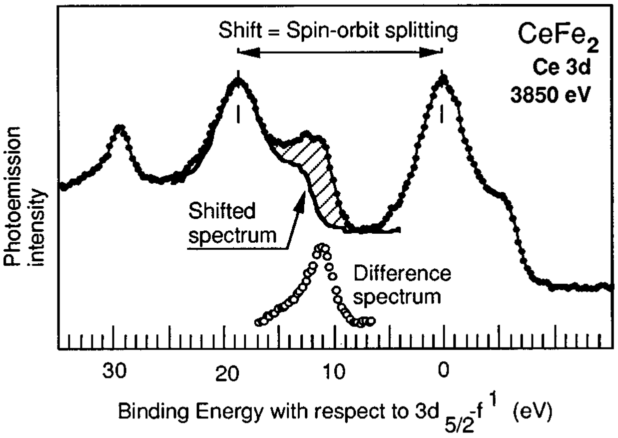

FIG. 4. The procedure to isolate the Ce-$3d_{5/2}$-f^0 contribution in the photoemission spectra (open dots in the bottom). See the text for an explanation. The spectra refer to $CeFe_2$.

A. Extraction of the f^0, f^1, and f^2 weights from a single spectrum

In order to extract the total f^0, f^1, and f^2 weights (surface+bulk) from a single spectrum we will follow an approach relying upon a very limited set of assumptions. Since this step is similar to what is already outlined in Ref. 13 we cover only some relevant points.

Determination of f^0. The Ce $3d_{3/2}$-f^0 peak is very well seen (around -30 eV in Fig. 1) and its area is obtained very easily. An independent measurement of the Ce$3d_{5/2}$-f^0 peak area is done as follows. In the $3d_{5/2}$-f^0 region there is also a contribution from the $3d_{3/2}$-f^2 contribution which can be eliminated as in Fig. 4. The measured spectrum is superimposed to the same spectrum shifted by the $3d$ spin-orbit splitting and rescaled by the statistical branching ratio (original spectrum given by the black dots and shifted spectrum by the heavy line). *Without making any assumption* the two spectra coincide very well, as they must, in the $3d_{3/2}$-f^1 region so that the shaded area between the two curves is due exclusively to the $3d_{5/2}$-f^0 contribution. The difference spectrum in the bottom of Fig. 4 (open points) gives the $3d_{5/2}$-f^0 line with a shape in good agreement with the $3d_{3/2}$-f^0 and an area consistent with the branching ratio. Thus two independent determinations of f^0 give consistent values. The accuracy of the $3d_{5/2}$-f^0 weight at 3850 eV is about 5%.

Determination of f^2 *and* f^1. This is based on $3d_{5/2}$ photoemission (Fig. 5). The evolution of the two high energy spectra (2660 and 3880 eV) measured in strictly comparable conditions is due to the small but measurable increase of the f^2 component when the spectra become more bulk sensitive as shown in Fig. 5(a) giving the Ce$3d_{5/2}$ spectra from $CeFe_2$ at 3850 eV and at 2660 eV normalized to the same peak height. The difference curve (shown at the bottom multiplied by a factor of 5) due to the f^2 increase defines rather well, in spite of the statistical noise, the experimental f^2 line shape, which is obtained by a polynomial fit (heavy line). In this way no assumption is made about the line shape, which comes directly from the experiment. The f^2 line shape is used in Fig. 5(b) to decompose the spectrum at 3850 eV. The f^2 peak is subtracted from the spectrum by finding the weight needed to obtain a difference curve representing f^1 free of undershoots and of oscillations, i.e., having a mono-

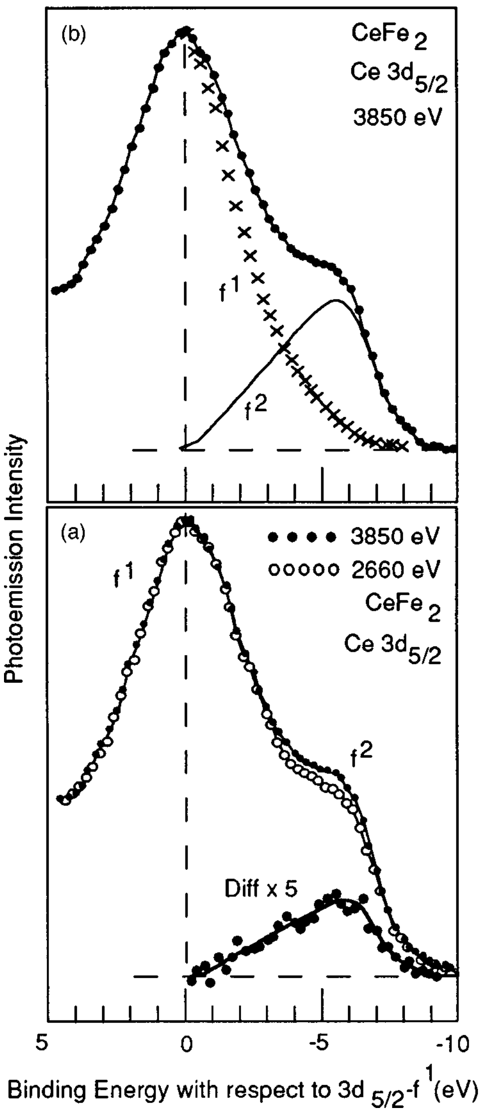

FIG. 5. The procedure to isolate the Ce $3d_{5/2}$-f^1 and $3d_{5/2}$-f^2 contributions in the photoemission spectra. See the text for an explanation. The spectra refer to $CeFe_2$. In (a) the spectrum at the bottom (black dots) defines the experimental lineshape of the f^2 contribution. (b) gives the optimized decomposition of the measured spectrum at 3880 eV (black dots) in the f^2 contribution (thin line) and in the f^1 contribution (crosses).

tonic variation of the first derivative and a simple oscillation of the second derivative. All these conditions are very restrictive and allow us to obtain the best result given by the crosses in panel *B* of Fig. 5. The difference between the spectra at 3850 and 2660 eV is small so that the background in the $3d_{5/2}$-f^2 region is basically the same in the two cases and the f^2 line shape is independent of any assumption on the background. This has been tested evaluating f^2 either in the spectra without the background subtraction or in the spectra after integral background subtraction done as explained in detail in Ref. 2 (see Fig. 1, $CeFe_2$). On the other hand, the intensity of f^1 is meaningful only after background subtraction and this introduces some uncertainty in f^1 on top of those coming from the f^2 subtraction. We have done extensive sensitivity tests of the whole procedure to the variation of the parameters including different ways of subtracting f^2. The more significant test was based on the use of spectra having different statistical fluctuations obtained by discarding at random a fraction (typically 30%) of the sweeps and by repeating the whole procedure. We found about 8–10 % uncertainty in f^2 and 5% in f^1.

B. Determination of f^0, f^1, and f^2 in the bulk spectral function

The kinetic energy dependence of the measured weights can be used to obtain the bulk values of f^0 and f^2 (and thus of f^1), i.e., the values one would measure in an ideal photoemission experiment sensitive only to the bulk. This is understood on the basis of the following arguments valid in the asymptotic limit $(s/L)\ll 1$ where $[1-\exp(s/L)]\cong(s/L)$. In this case it is legitimate to include all surface effects in a single term without distinguishing between surface and subsurface effects since they contribute to a small correction. The weight f of a given component (f indicates either f^0 or f^2) is the superposition of the surface f_s and of the bulk f_b contributions with bulk and surface weighting signals i_b, i_s, and $i_b+i_s=1$ so that

$$f=f_b i_b+f_s i_s=f_b(1-s/L)+f_s(s/L)=f_b-(s/L)(f_b-f_s), \tag{1}$$

where $(f_b-f_s)>0$ since the surface is γ like. Thus f is a linear decreasing function of $(1/L)$. If the dependence of the escape depth on the kinetic energy E_k is given by $L=f(E_k)$ the measured values must give in the asymptotic regime a linear plot as a function of $[1/f(E_k)]$. In the high kinetic-energy regime the escape depth[26,27] is well fitted by a simple power law $L=A\cdot(E_k)^\alpha$ with A and α constants so that formula (1) becomes

$$f=f_b-B\beta \tag{2}$$

with

$$B=(s/A)(f_b-f_s) \quad \text{and} \quad \beta=1/(E_k)^\alpha. \tag{3}$$

A plot of the measured values in the asymptotic regime is linear in the variable $\beta=1/(E_k)^\alpha$ with slope B given by Eq. (3) and with increasing bulk sensitivity at smaller β (higher kinetic energies).

At the beginning one finds the best exponent α linearizing the plot, which is $\alpha=1/2$ in agreement with the known square-root dependence of the escape depth in the high-energy range.[26,27] This is a strong support for the accuracy of the data treatment and is shown in Fig. 6 summarizing the measured values of f^0 and f^2 in $CeFe_2$ as a function of $\beta=1/(E_k)^{1/2}$.

The second step is the extraction of the f^0, f^1, and f^2 bulk values from the graph of Fig. 6. It is intuitive to extrapolate the trend to infinite kinetic energy ($\beta=0$) corresponding to complete bulk sensitivity as given by the thin lines in Fig. 6. As a matter of fact, this is not an artist extrapolation but is done iteratively up to self-consistency on the basis of the above expressions. A first extrapolation of the three points at lower β gives initial values of f_b^0 and of f_b^2. With these values one obtains from the definition of B the ratio η of the slopes of the two lines and a new fitting is done with this constraint, giving new bulk values. In order to determine η we used surface values f_s^0 and f_s^2 equal to the f^0

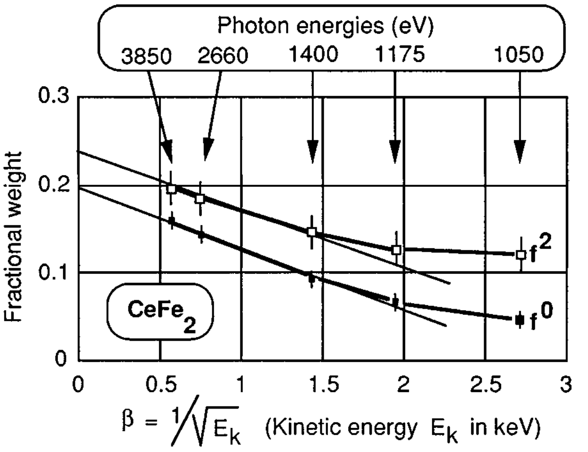

FIG. 6. Plot of the measured spectral weights f^0 and f^2 in $CeFe_2$ at different photon energies vs the inverse of the square root of the kinetic energy in the photoemission spectra. The thin lines fit the values belonging to the asymptotic regime in which the escape depth increases with the square root of the photoelectron kinetic energy. The extrapolation to zero gives the values in an ideal experiment having perfect bulk sensitivity (see the text).

and f^2 values in the measured spectrum of the γ-like compound Ce_7Ni_3 since in this case the bulk and surface parameters are similar.[28] One reaches self-consistency already in the second iteration showing that the procedure is intrinsically safe. Again this comes from the fact that the extrapolation effect is small. For this reason no more data points are needed at different photon energies. The results of the extrapolation (about 17% increase of f^0 and f^2 with respect to the spectrum at $h\nu = 3850$ eV) are consistent with an independent evaluation based on the available information on the surface thickness and on the escape depth anticipated in Sec. III and giving about 15% effect.

The extrapolation might seem naive since it implies that the law $L \div (E_k)^{1/2}$ is valid up to infinity. However, there are good physical reasons to believe in an asymptotic dependence close to the square root. The electron-electron scattering cross section in the high-energy limits approaches notoriously the $1/E_k^2$ low. At high excitation energies an almost free electron model is reasonable so that the total number of accessible states goes with $E_k^{3/2}$ leading to a mean free path proportional to $E_k^{1/2}$.

Having determined the extrapolated f^0 and f^2 values the bulk f^1 value is determined by the normalization condition $f^0 + f^1 + f^2 = 1$. The value of f^1 defined in this way is consistent with an independent extrapolation of the measured f^1 values done with the above approach.

The points at low kinetic energy (high β) in Fig. 5 deviate from the linear plot since they belong to the surface sensitive regime. The traditional XPS work with Al-$K\alpha$ x rays is within the asymptotic regime but in a situation where the data are still strongly influenced by the surface as already demonstrated in Refs. 4 and 6. Moreover, there are the difficulties mentioned above due to the superposition with the Ce-MNN Auger.[29] We stress that it is very difficult to increase drastically the bulk sensitivity with respect to the present experiment. In order to reduce by a factor of 2 the correction to the data in α-like compounds, one should increase the photon energy by approximately a factor of 4 entering an energy region extremely unfavorable for photoemission because of the cross section decrease and of the intensity loss due to the retardation factor in the electron spectrometer.

C. Accuracy of the results

As discussed above the extrapolation has little effect on the results and the accuracy of the results given in Table I is basically determined by the spectral weight decomposition [Sec. V A]. The main sources of uncertainty are the f^2 determination in the measured spectra which propagates into the f^1 value, and the background subtraction. In summary the overall uncertainties of the extrapolated bulk values of the Laves phases are ± 0.01 (f^0 components), ± 0.02 (f^2 components), and ± 0.03 (f^1 components). The inaccuracies combine to give always $f^0 + f^1 + f^2 = 1$.

VI. CONCLUSIONS

We have presented a rather detailed application of high-energy photoemission to Ce-3d spectroscopy with reference to the Laves phase sequence $CeFe_2$, $CeCo_2$, and $CeNi_2$, and to Ce_7Ni_3. The spectra with excitation near 4 keV are basically bulklike and this allowed us to introduce a new simple and effective way to extract reliable bulk information from the spectral functions. In the weakly hybridized γ-like Ce_7Ni_3 the spectra at high energies ($h\nu = 3850$ and 2660 eV) are essentially free of surface contributions within the sensitivity of the measurements. In the three Laves phases there is still about 15% surface contribution at the highest energy reached here (3850 eV). The bulk values have been discussed in connection with the available information on related systems. We have shown that the bulk hybridization in related compounds is likely to have been underestimated up to now and this suggests further high-energy photoemission work, which is now possible by exploiting third-generation synchrotrons. The measured bulk spectral weights have been discussed in connection with the trends of crystallographic properties in this Laves phase family. The present data have been also fitted qualitatively with a single impurity model thus recovering approximate ground-state properties which have been also discussed in connection with crystallographic data. Moreover, we have discussed the connection with the available information on an itinerant description by pointing out the inherent link between the calculated 4f bandwidth and the hybridization evaluated with the impurity model from the Ce-3d XPS.

ACKNOWLEDGMENTS

This paper has been partially supported by the INFM (Istituto Nazionale di Fisica della Materia) of Italy. One of us (M.S.) has been supported by the CNR (Consiglio Nazionale delle Ricerche of Italy). The authors are indebted to J. B. Goedkoop, J. Goulon, and A. Rogalev for the support during the experiments, in particular during the work at ID12A.

[1] O. Gunnarsson and K. Schönhammer, in *Handbook of Physics and Chemistry of Rare Earths*, Vol 10, edited by K. A. Gschneider, Jr., L. Eiring, and S. Hüfner (Elsevier, Amsterdam, 1987), p. 103, and references therein.

[2] J. W. Allen, S. J. Oh, O. Gunnarsson, K. Schönhammer, M. B. Maple, M. S. Torikachvili, and I. Lindau, Adv. Phys. **35**, 275 (1986), and references therein.

[3] D. Malterre, M. Grioni, and Y. Baer, Adv. Phys. **45**, 299 (1996), and references therein.

[4] C. Laubshat, E. Weschke, C. Holtz, M. Domke, O. Strebel, and G. Kaindl, Phys. Rev. Lett. **65**, 1639 (1990).

[5] E. Weschke, C. Laubshat, T. Simmons, M. Domke, O. Strebel, and G. Kaindl, Phys. Rev. B **44**, 8304 (1991).

[6] L. Z. Liu, J. W. Allen, O. Gunnarsson, N. E. Christensen, and O. K. Andersen, Phys. Rev. B **45**, 8934 (1992).

[7] J. Vogel, H. Magnan, J. P. Kappler, G. Krill, and D. Chandesris, J. Electron Spectrosc. Relat. Phenom. **76**, 735 (1995).

[8] O. Eriksson, L. Nordström, M. S. S. Brooks, and B. Johansson, Phys. Rev. Lett. **60**, 2523 (1988).

[9] L. Severin and B. Johansson, Phys. Rev. B **50**, 17 886 (1994).

[10] J. C. Fuggle, F. U. Hillebrecht, J.-M. Esteva, R. C. Karnatak, O. Gunnarsson, and K. Schönhammer, Phys. Rev. B **27**, 4637 (1983); J. C. Fuggle, F. U. Hillebrecht, Z. Zolnierek, R. Lässer, Ch. Freiburg, O. Gunnarsson, and K. Schönhammer, *ibid.* **27**, 7330 (1983).

[11] The insertion device is a helical undulator producing circularly polarized light [see P. Elleaume, J. Synchrotron Radiat. **1**, 19 (1994), and references therein]. In the present case there is no quantization axes and the circular polarization is immaterial.

[12] J. Goulon, N. B. Brookes, C. Gauthier, J. B. Goedkoop, C. Goulon-Ginet, M. Hagelstein, and A. Rogalev, Physica B **208-209**, 199 (1995).

[13] L. Braicovich, L. Duo', P. Vavassori, and G. L. Olcese, Surf. Sci. **331-333**, 782 (1995).

[14] B. Kierren, F. Bertran, T. Gourieux, N. Witkowski, D. Malterre, and G. Krill, Phys. Rev. B **53**, 5015 (1996).

[15] G. Chiaia, S. De Rossi, L. Duo', P. Vavassori, F. Ciccacci, G. L. Olcese, and I. Lindau, Surf. Sci. **357-358**, 293 (1996); G. Chiaia, P. Vavassori, L. Duo', L. Braicovich, M. Qvarford, and I. Lindau, *ibid.* **331-333**, 1229 (1995).

[16] For this reason there is no point in comparing with the pioneering work on conventional Ce-$3d$ XPS on $CeCo_2$ and $CeNi_2$ (Ref. 10).

[17] L. Duo', P. Vavassori, L. Braicovich, and G. L. Olcese, Phys. Rev. B **51**, 4751 (1995).

[18] $CeIr_2$ ($MgCu_2$-type Laves phase) has a lattice parameter equal to 7.573 Å i.e., about 5.7% greater than in $CeCo_2$ (7.161 Å) while the Ir-$5d$ wave functions in the isolated atom are much more expanded than the Co-$3d$ wave functions (about 30%) due to the radial zeros in the $5d$ functions. In fact, the distance needed to reach 1/10 of the peak value of the atomic wave function is 2.20 Å in Ir and 1.69 Å in Co. This strongly suggests a greater hybridization in $CeIr_2$.

[19] B. Kierren, F. Bertran, T. Gourieux, D. Malterre, and G. Krill, Europhys. Lett. **33**, 35 (1996).

[20] J. J. Joyce, A. J. Arko, J. M. Lawrence, P. C. Canfield, Z. Fiesk, R. J. Bartlett, and J. D. Thompson, Phys. Rev. Lett. **68**, 236 (1992).

[21] A. B. Andrews, J. J. Joyce, A. J. Arko, J. D. Thompson, J. M. Lawrence, and J. C. Hemminger, Phys. Rev. B **51**, 3277 (1995).

[22] E. Weshke, C. Laubschat, R. Ecker, A. Höhr, M. Domke, G. Kaindl, L. Severin, and B. Johansson, Phys. Rev. Lett. **69**, 1792 (1992).

[23] D. Malterre, M. Grioni, Y. Baer, L. Braicovich, L. Duo', P. Vavassori, and G. L. Olcese, Phys. Rev. Lett. **73**, 2005 (1994).

[24] In the first fittings on these compounds (typically $CeCo_2$ in Ref. 10 and $CeNi_2$ in Ref. 2) the parameters are strongly influenced by the fact that the surface and the bulk contributions are not disentangled so that they cannot be used as a starting point in the present analysis and cannot be compared with the present parameters.

[25] O. Gunnarsson and O. Jepsen, Phys. Rev. B **38**, 3568 (1988).

[26] M. P. Seah and W. A. Dench, Surf. Interface Anal. **1**, 2 (1979).

[27] S. Tanuma, C. J. Powell, and D. R. Penn, Surf. Sci. **192**, L849 (1987).

[28] The accuracy of this assumption is not at all critical since f_s^0 and f_s^2 are small numbers and have very little effect on the procedure.

[29] In order to clarify this point we have analyzed also the data measured in the present synchrotron radiation experiment at the same energy as Al-$K\alpha$. The results are obviously similar to those summarized in Fig. 6 but do not coincide exactly with the trend due to the specific difficulties encountered at this photon energy. The data points at the Al-$K\alpha$ energy are about 6–8 % out of the thin lines of Fig. 6.